

# Pushing Inkjet Printing to W-band: An all-printed 90-GHz beamforming array

John Kimionis\*, Shahriar Shahramian\*, Yves Baeyens\*, Amit Singh\*, and Manos M. Tentzeris†

\*Nokia - Bell Labs

600 Mountain Ave, Murray Hill, NJ 07974

Email: {ioannis.kimionis, shahriar.shahramian, yves.baeyens, amit.singh}@nokia-bell-labs.com

†Georgia Institute of Technology

85 5th St NW, Atlanta, GA, 30332

Email: etentze@ece.gatech.edu

**Abstract**—In this work, the inkjet printing process is refined to push the capabilities of additive manufacturing up to the W-band (75–110 GHz). The idiosyncrasies of inkjet printing on polymer dielectric materials are fully taken into account, to mitigate the effect of excessive ink spreading which results in RF circuit detuning and performance deterioration. The developed process enables the fabrication of the very first inkjet-printed 90 GHz array on a flexible substrate, featuring 5 elements and a 11.3 dBi gain. High fabrication accuracy has been achieved without using any specialized surface treatment equipment, effectively reducing the baseline equipment for mmWave system fabrication to a single inkjet printer and a convection oven. The proof-of-concept array's form factor will allow integration with beam-forming networks; as an example, a miniaturized  $4 \times 4$  Butler matrix is designed with the achieved fabrication space constraints which opens the way for the first fully-printed beamforming arrays operating in W-band with significant fabrication cost savings.

**Index Terms**—mmWave, inkjet printing, passive arrays, beam-forming, Butler matrix

## I. INTRODUCTION

Antenna arrays have been typically associated with large, bulky, and special-purpose systems, such as synthetic aperture radar, military communications, or wireless backhaul. Nevertheless, they are now introduced to consumer/commercial electronics, due to the need for high-speed data transfer between devices and access points. Miniaturization of such arrays is crucial to enable integration with mobile sensors, wearable systems, and smart home gateways, which gives the rationale for dramatically increasing the frequency of operation. The 75–110 GHz band (W-band) is a great candidate for short-distance, ultrafast-datarate links, since it can support bit rates of multiple gigabits per second within a small fractional bandwidth. However, W-band systems generally pose high manufacturing costs due to the fabrication accuracy and low-loss materials required. *Inkjet printing* has been successfully utilized to offer low-cost solutions in RF system fabrication, including passive and active antenna arrays, but has until now been targeted to lower operation frequencies. In [1], an active printed antenna array was presented with beamforming capabilities, operating at 6 GHz. In [2], inkjet-printed 24 GHz arrays enabled mm-Wave digital backscatter transmission. The combination of additive manufacturing technologies [3] and spectral-efficient backscatter radio [4] will offer a jointly

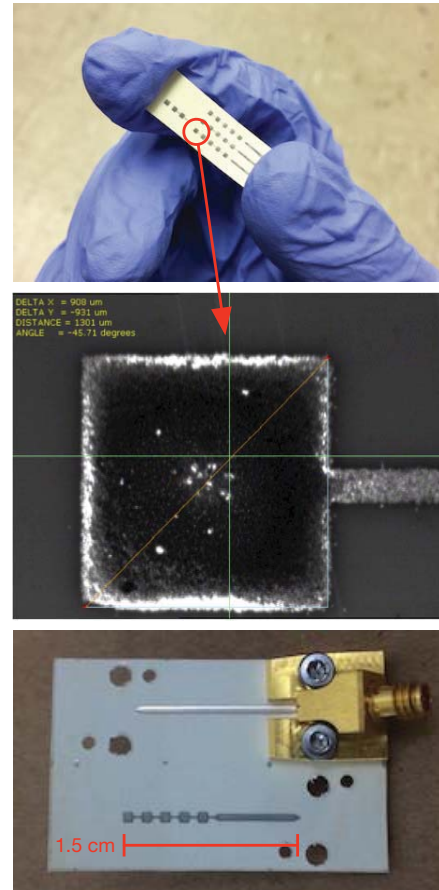


Fig. 1. Top: Inkjet-printed W-band array prototypes. Center: Microphotograph of W-band array patch element. Bottom: 1.0-mm top-launch connector attached to prototype's calibration line.

optimized solution, in terms of cost and power, for mm-Wave Internet-of-Things (IoT) sensors and communicators. Leveraging such technologies to W-band will offer high levels of miniaturization and integration capabilities. In this work, inkjet printing is used to demonstrate for the first time the low-cost fabrication of W-band RF systems, with notable accuracy and without the use of specialized equipment for material treatment.

## II. INKJET PRINTING FOR THE W-BAND

Inkjet printing has been highly utilized for UHF electronics, especially radio frequency identification (RFID) tags operating at sub-GHz frequencies, where fabrication tolerances can be high, without significantly affecting the performance of antennas or transmission lines (e.g. [5]). Recent efforts utilized inkjet printing for 24 GHz on-chip applications [6], or even inkjet-printed interconnects, up to 40 GHz ([7]). As the frequency of operation increases, fabrication becomes more challenging, due to incompatibilities between the metal inks (typically silver nanoparticles - SNP) surface tension and the substrates' surface energy. Inkjet printing on high-frequency, low-loss substrates such as liquid crystal polymer (LCP) often results in ink spreading (“bleeding”) which locally widens transmission lines, or shorts adjacent conductive traces. Ink adhesion and drop formation can be improved by employing specialized surface treatment equipment such as as UV-ozone or Oxygen-plasma cleaners.

For this work, no surface treatment equipment has been utilized. The substrate (Rogers Ultralam 3850HT LCP,  $\epsilon_r = 3.14$ ,  $\tan \delta = 0.002$ ) preparation only involves *pre-baking* the LCP at 150° C for at least 30 minutes, before it is used as a carrier for printed SNP patterns printed with a Dimatix DMP-2831 printer and annealed/sintered in a convection oven. This pre-baking step has been found to have a tremendous impact in the inkjet drop formation on the substrate, with achievable feature sizes as small as 40  $\mu\text{m}$ , for 4 stacked layers of silver ink. This creates a foundation for successful fabrication of demanding W-band structures.

Ink spreading results in larger electrical sizes compared to the original design, and the effects of that are prominent in mmWave frequencies. For this work, post-fab simulations have been performed, that take into account the resulting trace widths after printing and sintering. Then, any subsequent design to be printed is pre-shrunk (typically by 20  $\mu\text{m}$ ) before it is printed. The method has been tested with a fine-pitch CPW structure (40  $\mu\text{m}$  gaps) that has been printed and characterized on a probe station with 150  $\mu\text{m}$  ground-signal-ground (GSG) probes. The predicted (modeled and simulated) structure behavior is shown along with the measurements of different printed batches in Fig. 2), where a reasonable agreement can be seen. The substrate and pattern preparation techniques can then be used to implement more complex mmWave structures.

## III. PROVING THE CONCEPT: W-BAND ANTENNA ARRAY

As a proof-of-concept, a 5-element, series-fed patch antenna array has been implemented, with a center frequency of 90 GHz. The fabricated patch elements have dimensions of 908  $\times$  930  $\mu\text{m}$ , with 80  $\mu\text{m}$ -wide feedlines between the patches (Fig. 1). The element spacing is approximately one wavelength in the LCP medium, which yields a directivity of 13.7 dBi and a realized gain of 11.3 dBi, as shown in Fig. 3. To achieve accurate fabrication, the ink spread on the substrate due to LCP’s surface energy and multiple silver layer stacking is taken into account in the pattern that is printed;

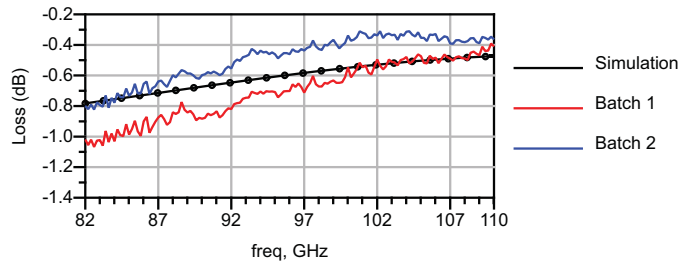
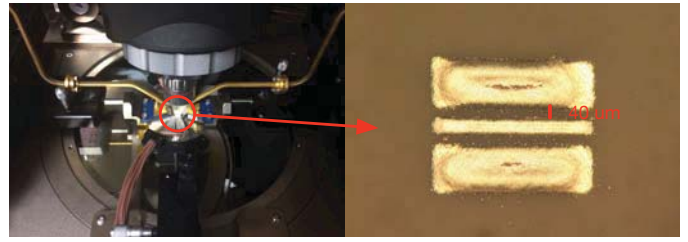


Fig. 2. Probe-station measurements of 1 mm-long CPW structure along with predicted performance of inkjet-printed silver lines on LCP.

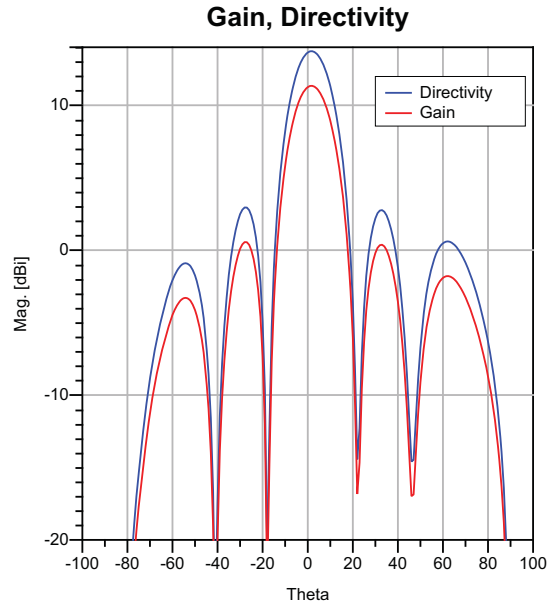


Fig. 3. 1  $\times$  5 printed W-band array directivity and realized gain at 90 GHz.

prior to printing, all outer dimensions (patches and feedlines perimeters) are shifted inwards by 20  $\mu\text{m}$ . Then, the printing process described in Sec. II is followed.

A top-launch 1.0-mm coaxial connector is screwed on the LCP substrate, where mounting holes have been drilled (Fig. 1). A 5 mm-long 50  $\Omega$  microstrip line connects the coaxial connector to the antenna array, while an equal width 10 mm-long microstrip is printed alongside the array for de-embedding purposes. The printed array is connected to a vector network analyzer (VNA) equipped with 75–110 GHz frequency extenders. A 20 dBi WR-10 reference horn antenna is connected to the second port of the VNA to establish a

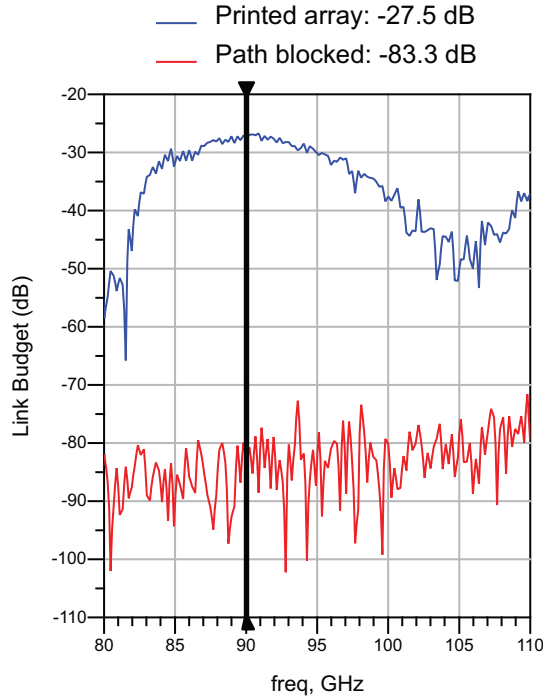
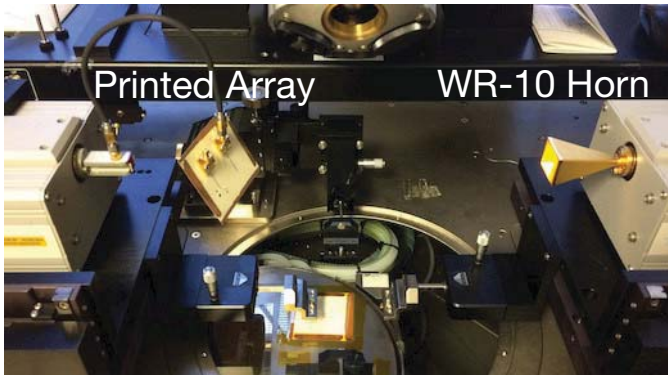


Fig. 4. Top: wireless measurement setup using W-band frequency extenders. Bottom: Link budget measurement with inkjet-printed array and reference WR-10 horn.

wireless link with an antenna-to-antenna separation of approximately 20 cm. The expected link budget (free space path loss minus the transmit and receive antenna gain values) at 90 GHz with a 11.3 dBi printed array and an 20 dBi horn at 20 cm separation is -26.25 dB, assuming a line-of-sight link. The VNA-measured link budget is shown in Fig. 4 where a -27.5 dB value can be seen at the center frequency. For comparison, a -83.3 dB value is obtained when the path between the two antennas is blocked with a metal plate. The measured value of -27.5 dB at the boresight of the printed array is an appealing result regarding its performance, given the low cost of inkjet printing fabrication.

#### IV. THE BIG PICTURE: ALL-PRINTED BUTLER MATRIX

The promising performance of the proof-of-concept inkjet-printed  $1 \times 5$  W-band array calls for a larger-scale array implementation with beam steering capabilities. A preliminary

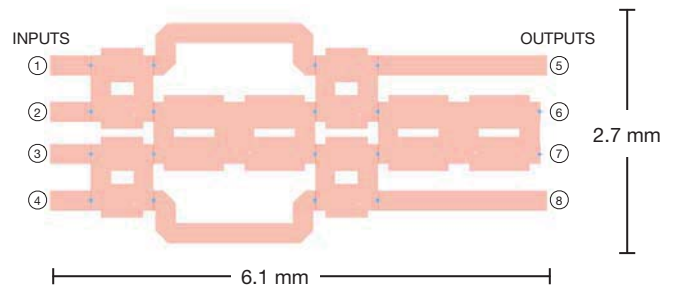


Fig. 5. Proposed Butler matrix layout.

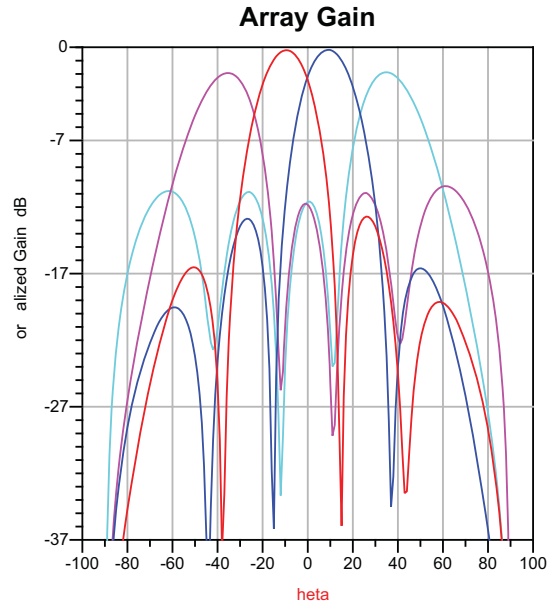


Fig. 6. Expected  $4 \times 5$  array gain with Butler matrix excitation.

$4 \times 4$  Butler matrix has been designed, with the primary constraints of a) miniaturization to reduce the printing area, as well as conductive losses, b) respecting the minimum clearance distance of  $40 \mu\text{m}$  that can be achieved on the pre-baked LCP without the use of other surface modification techniques. The matrix has the approximate dimensions of  $6.1 \times 2.7 \text{ mm}$ , and consists of  $90^\circ$  branchline couplers to keep the structure purely planar (Fig. 5). The output (ports 5 through 8) phase differences of the passive beamforming network are obtained with full-wave simulation, taking into account the SNP conductive and LCP dielectric losses, and are summarized in Table I.

TABLE I  
BUTLER MATRIX OUTPUT PHASE DIFFERENCES

	Port 1 Excitation	Port 2 Excitation	Port 3 Excitation	Port 4 Excitation
$\phi_8 - \phi_7$	$-33.94^\circ$	$149.41^\circ$	$-125.4^\circ$	$37.66^\circ$
$\phi_7 - \phi_6$	$-35.14^\circ$	$127.3^\circ$	$-127.09^\circ$	$35.91^\circ$
$\phi_6 - \phi_5$	$-36.29^\circ$	$126.02^\circ$	$-149.47^\circ$	$33.81^\circ$

By placing four parallel  $1 \times 5$  90-GHz arrays with  $\lambda$  spacing

and driving each array with a respective Butler matrix output port, the total array gain scanning angle will be changed, depending on the excitation port. In Fig. 6, the predicted gain versus scanning angle of the full  $4 \times 5$  array is shown. When Port 1 through Port 4 is excited, the main array beam changes from  $-35^\circ$  to  $35^\circ$ , with the first sidelobes being below -11 dB.

## V. CONCLUSION

This paper presented the first inkjet-printed W-band antenna array operating in the 85–95 GHz band. With a simplified printing process allowing for accurate  $80 \mu\text{m}$ -wide trace fabrication and  $40 \mu\text{m}$ -wide gaps without specialized surface modification equipment, the potential for using inkjet printing for challenging mmWave structures has been demonstrated. The next steps for this work will include the integration of multiple printed linear antenna arrays with an all-printed Butler matrix to create the first all-printed beam steering-capable W-band arrays, with results to be presented at the conference.

## REFERENCES

- [1] H. Subbaraman, D. T. Pham, X. Xu, M. Y. Chen, A. Hosseini, X. Lu, and R. T. Chen, "Inkjet-Printed Two-Dimensional Phased-Array Antenna on a Flexible Substrate," *IEEE Antennas Wirel. Propag. Lett.*, vol. 12, pp. 170–173, 2013. [Online]. Available: <http://ieeexplore.ieee.org/document/6450043/>
- [2] J. Kimionis, A. Georgiadis, and M. M. Tentzeris, "Millimeter-wave backscatter: A quantum leap for gigabit communication, RF sensing, and wearables," in *2017 IEEE MTT-S Int. Microw. Symp.* IEEE, jun 2017, pp. 812–815. [Online]. Available: <http://ieeexplore.ieee.org/document/8058702/>
- [3] I. Gibson, D. W. Rosen, and B. Stucker, *Additive manufacturing technologies*. New York: Springer, 2010.
- [4] J. Kimionis and M. M. Tentzeris, "Pulse Shaping: The Missing Piece of Backscatter Radio and RFID," *IEEE Trans. Microw. Theory Tech.*, vol. 64, no. 12, pp. 4774–4788, dec 2016. [Online]. Available: <http://ieeexplore.ieee.org/document/7755817/>
- [5] H. He, J. Tajima, L. Sydanheimo, H. Nishikawa, L. Ukkonen, and J. Virkki, "Inkjet-printed antenna-electronics interconnections in passive UHF RFID tags," in *2017 IEEE MTT-S Int. Microw. Symp.* IEEE, jun 2017, pp. 598–601. [Online]. Available: <http://ieeexplore.ieee.org/document/8058638/>
- [6] F. A. Ghaffar, S. Yang, H. M. Cheema, and A. Shamim, "A 24 GHz CMOS oscillator transmitter with an inkjet printed on-chip antenna," in *2016 IEEE MTT-S Int. Microw. Symp.* IEEE, may 2016, pp. 1–3. [Online]. Available: <http://ieeexplore.ieee.org/document/7540081/>
- [7] B. K. Tehrani, B. S. Cook, and M. M. Tentzeris, "Inkjet-printed 3D interconnects for millimeter-wave system-on-package solutions," in *2016 IEEE MTT-S Int. Microw. Symp.*, no. August. IEEE, may 2016, pp. 1–4. [Online]. Available: <http://ieeexplore.ieee.org/document/7540084/>